RESEARCH ARTICLE

STRUCTURAL BIOLOGY

Structure-based discovery of nonhallucinogenic psychedelic analogs

Dongmei Cao[1]†, Jing Yu[1]†, Huan Wang[2]†, Zhipu Luo[3]†, Xinyu Liu[4]†, Licong He[1], Jianzhong Qi[1], Luyu Fan[1], Lingjie Tang[1], Zhangcheng Chen[1], Jinsong Li[4], Jianjun Cheng[2]*, Sheng Wang[1]*

Drugs that target the human serotonin 2A receptor (5-HT_{2A}R) are used to treat neuropsychiatric diseases; however, many have hallucinogenic effects, hampering their use. Here, we present structures of 5-HT_{2A}R complexed with the psychedelic drugs psilocin (the active metabolite of psilocybin) and D-lysergic acid diethylamide (LSD), as well as the endogenous neurotransmitter serotonin and the nonhallucinogenic psychedelic analog lisuride. Serotonin and psilocin display a second binding mode in addition to the canonical mode, which enabled the design of the psychedelic IHCH-7113 (a substructure of antipsychotic lumateperone) and several 5-HT_{2A}R β-arrestin–biased agonists that displayed antidepressant-like activity in mice but without hallucinogenic effects. The 5-HT_{2A}R complex structures presented herein and the resulting insights provide a solid foundation for the structure-based design of safe and effective nonhallucinogenic psychedelic analogs with therapeutic effects.

Serotonin, or 5-hydroxytryptamine (5-HT), is a neurotransmitter that modulates most human behavioral processes (*1*), and drugs that target serotonin receptors are widely used in psychiatry and neurology (*1*). Among these drugs, the serotonergic hallucinogens (psychedelics) alter consciousness and may have potential for drug development (*2*–*5*). For example, D-lysergic acid diethylamide (LSD) and psilocybin have shown promise for addressing many neuropsychiatric diseases (*2*). Preliminary open-label trials have shown their potential for symptom alleviation in mood disorders and anxiety in the terminally ill (*2*, *6*), and recently completed phase 2 clinical trials showed that psilocybin is a viable alternative to current antidepressant medications (*7*). The therapeutic effects of LSD and psilocybin appear to be both rapid and enduring (*6*, *8*–*10*).

Previous studies have identified oleamide (an endogenous fatty acid amide) in the cerebrospinal fluid of sleep-deprived cats and rats and demonstrated that it was able to potentiate human serotonin 2A receptor (5-HT_{2A}R)–mediated signaling (*11*–*14*). This result suggested that abnormal sensitivity of 5-HT_{2A}R to oleamide and other endogenous fatty acids could be responsible for some aspects of psychiatric disorders, such as anxiety and depression. A lack of structural information of 5-HT_{2A}R with fatty acids limits our ability to undertake the structure-based design of safe and effective antidepressants. Additionally, although two recent studies have reported nonhallucinogenic psychedelic analogs with antidepressant-like behavior (*15*, *16*), it remains unclear how to rationally design such compounds, even with the 25 serotonin receptor structures in hand (*17*–*24*), and it is unclear whether the hallucinogenic effects of psychedelics are necessary for therapeutic effects (*2*, *7*–*10*).

[1]State Key Laboratory of Molecular Biology, Shanghai Institute of Biochemistry and Cell Biology, Center for Excellence in Molecular Cell Science, Chinese Academy of Sciences, University of Chinese Academy of Sciences, 320 Yueyang Road, Shanghai 200031, China. [2]iHuman Institute, ShanghaiTech University, 393 Middle Huaxia Road, Shanghai 201210, China. [3]Institute of Molecular Enzymology, School of Biology and Basic Medical Sciences, Soochow University, Suzhou, Jiangsu 215123, China. [4]State Key Laboratory of Cell Biology, Shanghai Institute of Biochemistry and Cell Biology, Center for Excellence in Molecular Cell Science, Chinese Academy of Sciences, University of Chinese Academy of Sciences, 320 Yueyang Road, Shanghai 200031, China.
***Corresponding author. Email: chengjj@shanghaitech.edu.cn (J.C.) and wangsheng@sibcb.ac.cn (S.W.)**
†These authors contributed equally to this work.

Lipid activation of 5-HT_{2A}R

Based on modeling and site-directed mutagenesis studies, tryptamine ligands, such as serotonin and psilocin, are predicted to bind to serotonin receptors in a similar manner to ergoline ligands (*3*, *19*, *23*). To investigate this, we compared the conformations of two ergoline-bound 5-HT_{2A}R structures (LSD and lisuride) with the serotonin- and psilocin-bound 5-HT_{2A}R complex structures (Fig. 1A and table S1). Recent structures of serotonin bound to 5-HT_{1A}R and 5-HT_{1D}R are reminiscent of structures of ergolines bound to serotonin receptors (*17*–*21*, *23*, *24*). In our structures with 5-HT_{2A}R, the ergoline moieties of LSD and lisuride are bound similarly to previous structures at the bottom of the orthosteric binding pocket (OBP) (*17*–*21*, *23*), but in contrast, the indole serotonin-psilocin core is located higher in the orthosteric pocket, closer to extracellular loop 2 (EL2) and the extracellular space, where they engage the extended binding pocket (EBP) of the receptor, which is occupied by the diethyl moiety of LSD and lisuride (*19*, *20*).

All of our 5-HT_{2A}R complex structures showed clear density maps occupying the previously identified side-extended pocket (SEP) (*22*) that could be best fit with monoolein, the lipid used in crystallization, which is structurally similar to oleamide (Fig. 1B and figs. S1A and S2A). In the serotonin-, psilocin-, LSD-, and lisuride-bound structures, the Fo-Fc omit maps allowed us to unambiguously define the binding pose of the monoolein glycerol group (Fig. 1B). Because of its high flexibility, the exact position of the alkyl chain could only be partially assigned (Fig. 1B and fig. S1A). However, all the glycerol groups of monoolein are inserted into the SEP in the serotonin-, psilocin-, LSD-, and lisuride-bound 5-HT_{2A}R structures. Compared with the LSD- and lisuride-bound complexes, the glycerol groups of monoolein are driven deep into the OBP in the structures of the serotonin- and psilocin-bound complexes (fig. S1B). Here, the deep insertion of monoolein may partially explain why serotonin and psilocin engage the EBP and not the OBP of the receptor (fig. S1B).

Our serotonin- and psilocin-bound structures show monoolein directly interacting with $S239^{5.43}$ and $S242^{5.46}$ (S, serine), which have been proposed as key residues in serotonin, dopamine, and adrenergic receptor activation (*23*, *25*, *26*) (fig. S1B). This suggested that binding of monoolein at the SEP might activate 5-HT_{2A}R. Based on calcium flux and β-arrestin2 recruitment assays (see methods), we found monoolein to be a modest G protein partial agonist without detectable β-arrestin2 activity and found that the 5-HT_{2A}R selective antagonist MDL100907 can block monoolein's G protein partial agonism (Fig. 1C and fig. S1C). We also tested monoolein in orthogonal β-arrestin2 association and $G_{q-\gamma}$, $G_{i1-\gamma}$, $G_{12-\gamma}$, $G_{i3-\gamma}$, $G_{15-\gamma}$, and $G_{z-\gamma}$ dissociation assays by bioluminescent resonance energy transfer (BRET) (*23*, *27*), which confirmed G protein partial agonism and no agonist activity in β-arrestin2 association (fig. S1, D and E). Among the different G protein signaling pathways, monoolein most robustly induced $G_{q-\gamma}$, $G_{i1-\gamma}$, and $G_{15-\gamma}$ dissociation assays (fig. S1E).

We found that oleamide, oleylethanolamide (OEA), and 2-oleoyl glycerol (2OG) also activated 5-HT_{2A}R–mediated G protein signaling and not β-arrestin2 activity (Fig. 1D and fig. S2, A and B). Conversely, oleic acid and oleoyl-L-α-lysophosphatidic acid (LPA) did not activate 5-HT_{2A}R–mediated signaling (fig. S2A). The 5-HT_{2A}R selective antagonist MDL100907 blocked the G protein partial agonism of these lipids (fig. S2C).

At position 5.42 (the key residue of OBP), a glycine residue is conserved only in the 5-HT_2 family among aminergic receptors (fig. S2D). This glycine allows the SEP to extend from

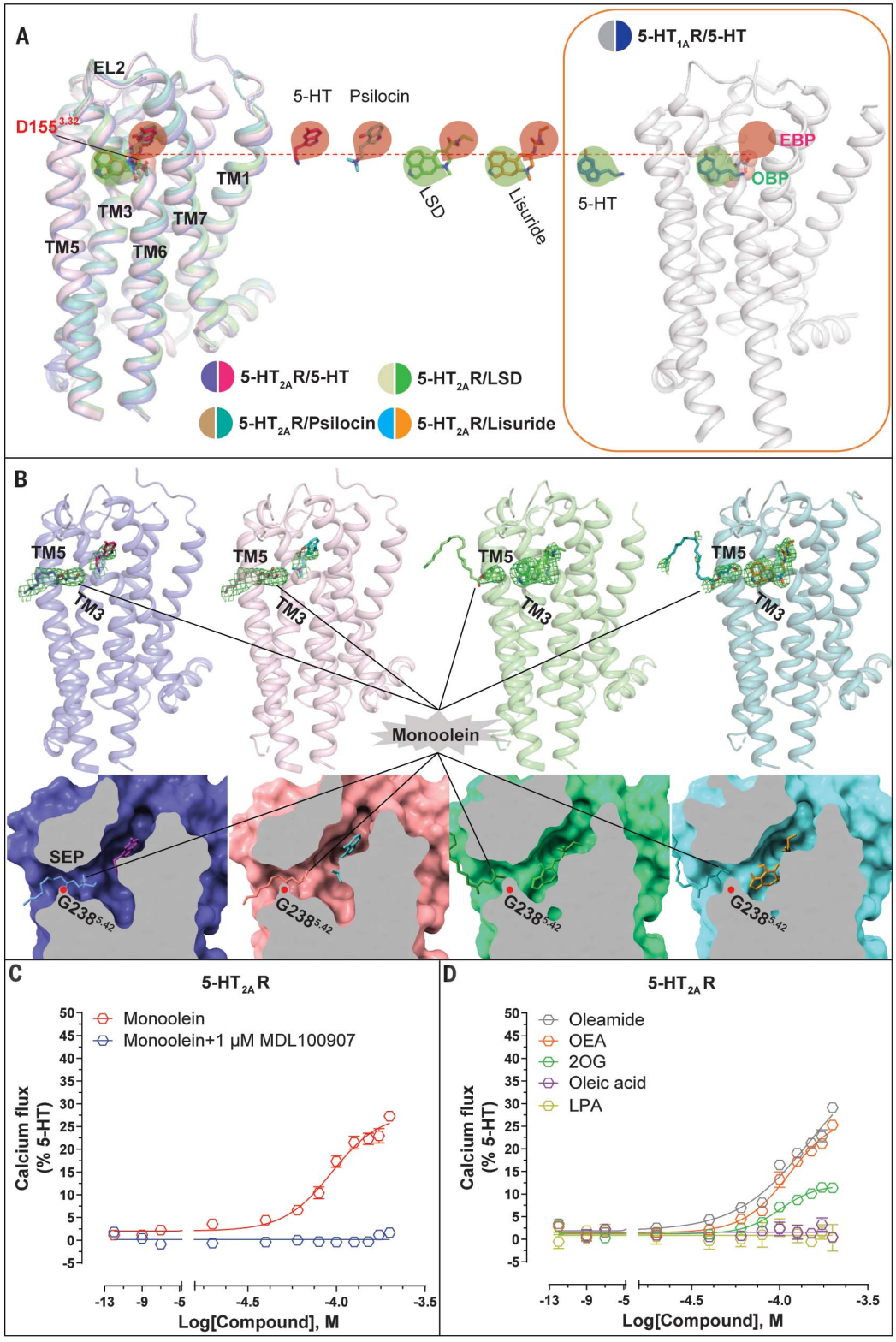

Fig. 1. Lipid regulation of 5-HT$_{2A}$R. (**A**) Overall view of 5-HT$_{2A}$R in complex with 5-HT, psilocin, LSD, and lisuride structures. (**B**) The bound monoolein in the SEP of 5-HT$_{2A}$R. Monoolein and the ligands are shown as sticks with omit electron density maps (Fo-Fc omit map) at the contour level of 3.0 σ. (**C**) Monoolein is a G protein–mediated calcium flux partial agonist in 5-HT$_{2A}$R. (**D**) 5-HT$_{2A}$R G protein calcium flux activity by oleamide, OEA, and 2OG. In all panels, the Ballesteros-Weinstein numbering is shown as superscript. In (C) and (D), error bars represent SEM (n = 3).

the OBP (Fig. 1B). Other aminergic receptors have an alanine, serine, cysteine, or threonine at this position and the side chain blocks the cavity (*22*). Introducing a G238$^{5.42}$S (G, glycine) substitution in 5-HT$_{2A}$R to mimic other 5-HT receptors abolished the agonist activity of the lipids but not of serotonin (fig. S2E). 5-HT$_{2B}$R and 5-HT$_{2C}$R have the conserved glycine, but structures show that the side chain of F$^{5.38}$ (F, phenyalanine) disrupts the SEP (*21*, *22*) (fig. S2F). As expected, lipids did not induce robust G protein signaling at 5-HT$_{2B}$R or 5-HT$_{2C}$R, or at other 5-HT receptors, such as 5-HT$_6$R and 5-HT$_7$R, where the glycine is not conserved (fig. S2G). These results provide a structural basis for the long-standing observation that 5-HT$_{2A}$R signaling is modulated by lipids (*11*–*14*).

Serotonin and psilocin have a second binding mode at 5-HT$_{2A}$R

Unlike previous docking results (*23*), our crystal structures showed that the indole core of serotonin or psilocin fits into a narrow cleft previously described as the EBP (*20*, *28*) that is lined mainly by hydrophobic side chains from residues in EL2 and transmembrane helices TM3, TM6, and TM7 (Fig. 2, A and B). Both ligands form a salt bridge between D155$^{3.32}$ (D, aspartic acid) and the terminal basic nitrogen of the molecules as well as an extra hydrogen bond between N352$^{6.55}$ (N, asparagine) and the hydroxyl group on the indole core. Mutagenesis of many of these contact residues to alanine reduced the affinity of serotonin and psilocin binding to 5-HT$_{2A}$R (table S2). We observed strong electron density at the top of OBP but no electron density at the bottom, which was previously shown to be the pocket of serotonin in 5-HT$_{1A}$R and 5-HT$_{1D}$R (*24*) (Fig. 1B and fig. S1A). However, alanine mutagenesis of residues at the bottom of the OBP that are implicated in serotonin binding in the 5-HT$_{1A}$R and 5-HT$_{1D}$R complex structures (*24*) also greatly affected serotonin and psilocin binding to 5-HT$_{2A}$R (table S2). A comparison of the previous published active 5-HT$_{2A}$R with our serotonin- and psilocin-bound 5-HT$_{2A}$R (*23*) shows that there is no obvious difference in the area of the actual ligand binding site (fig. S3, A and B). Thus, it appears that the alternative poses of serotonin and psilocin are compatible with the active state.

These findings suggested that serotonin and psilocin might adopt two different positions (OBP versus EBP) that could differentially affect receptor function. Accordingly, we mutated the key residues S239$^{5.43}$ and S242$^{5.46}$ for OBP, respectively, and W151$^{3.28}$ and L362$^{7.35}$ for EBP, respectively (W, tryptophan; L, leucine). Consistent with previous findings (*22*, *23*), S239$^{5.43}$A and S242$^{5.46}$A (A, alanine) substitutions substantially diminished serotonin and psilocin's agonism (fig. S3, C and D) and binding affinity (table S2), indicating that both agonists occupy the bottom of the OBP. The substitution of W151$^{3.28}$ or L362$^{7.35}$ with phenylalanine or alanine, which we predicted would dampen hydrophobic contacts with the indole core of serotonin and psilocin in the second pose, also substantially decreased or abolished agonist activity. Because lisuride and LSD occupy the EBP and OBP, all mutants also dampened the efficacy of lisuride and LSD. Importantly, the L362$^{7.35}$F substitution did not affect the potency of the ligands' G_q agonism, but it abolished psilocin's and lisuride's β-arrestin association (fig. S3, C and D). In all mutants, 5-HT$_{2A}$R expression levels were comparable to that of the wild type (fig. S3E). These results indicate that ligand recognition in the EBP, specifically at L362$^{7.35}$, affects ligand bias.

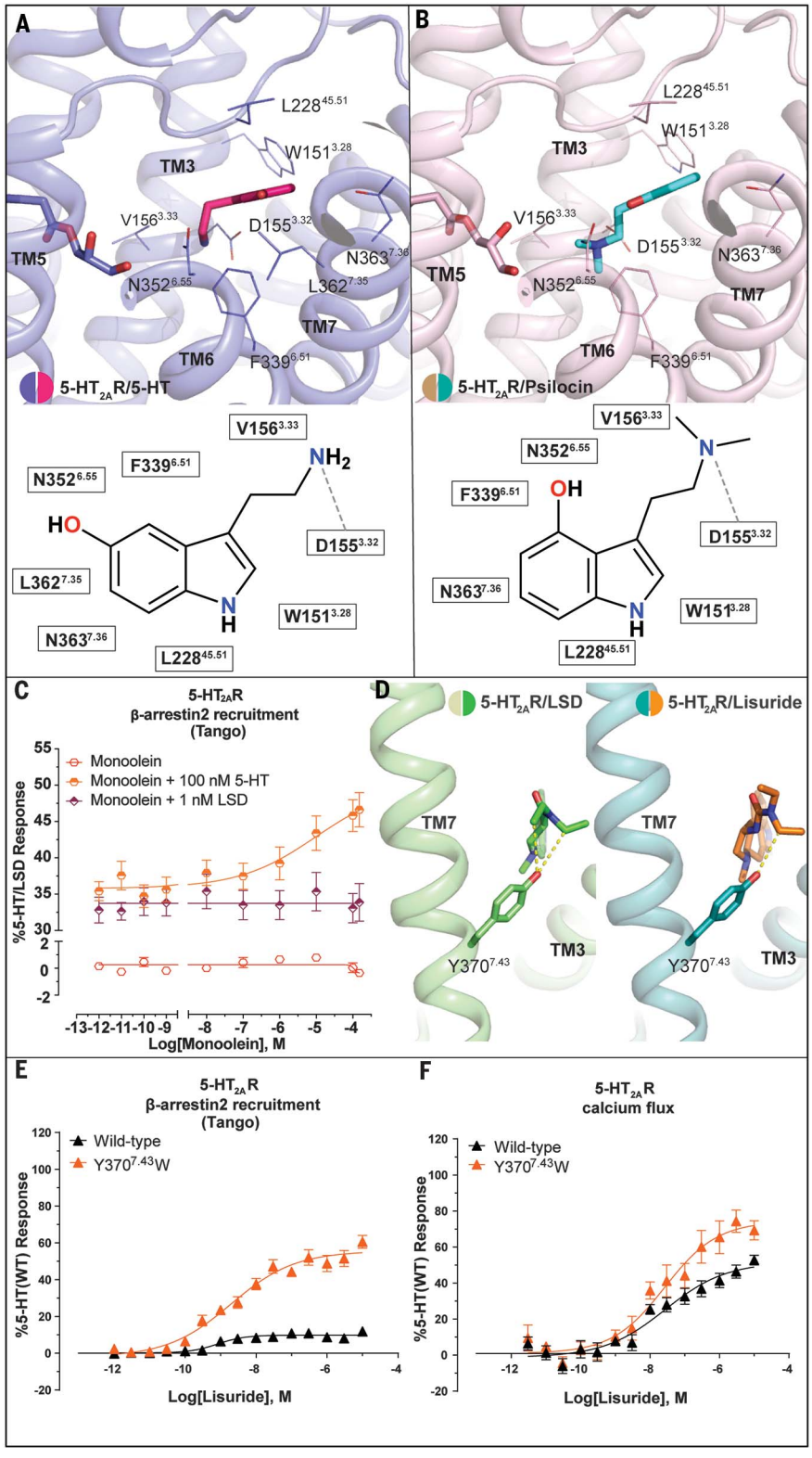

Fig. 2. EBP of 5-HT$_{2A}$R. (**A** and **B**) The second binding mode of 5-HT (A) and psilocin (B) with interaction residues at a 4.0-Å cut-off. Hydrogen bonds between D155$^{3.32}$ and the 5-HT or psilocin basic nitrogen are shown by a dashed line. V, valine. (**C**) Monoolein is a positive allosteric modulator of 5-HT$_{2A}$R–mediated β-arrestin2 recruitment (as measured by the Tango assay). (**D**) Comparison of the binding poses between LSD and lisuride at 5-HT$_{2A}$R. The specific contacts between Y370$^{7.43}$ and lisuride or LSD are shown with dashed lines. (**E** and **F**) Lisuride β-arrestin2 recruitment (E) and calcium flux (F) activity of the Y370$^{7.43}$W mutant (yellow) compared with wild-type 5-HT$_{2A}$R (black). In (C), (E), and (F), error bars represent SEM (n = 3).

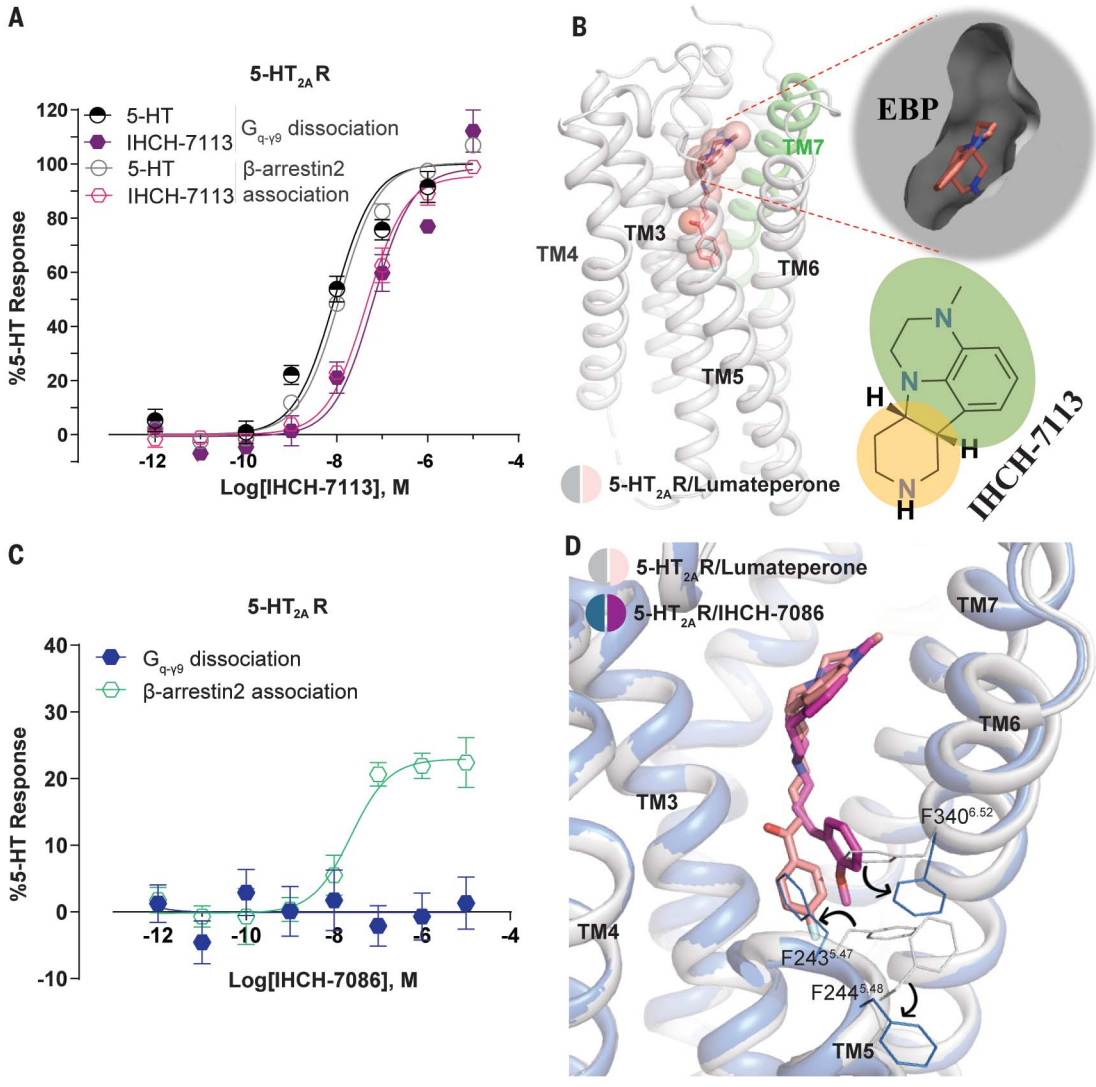

Fig. 3. Structure-guided design of 5-HT$_{2A}$R β-arrestin–biased agonists. (**A**) Normalized concentration-response studies for IHCH-7113 in 5-HT$_{2A}$R–mediated activation of $G_{q-\gamma9}$ dissociation and β-arrestin2 association as measured by BRET. (**B**) The lumateperone-bound 5-HT$_{2A}$R complex structure highlights the potential binding pose of IHCH-7113 at the EBP. (**C**) Profiling of IHCH-7086 for ligand bias showing β-arrestin2 association partial agonist activity but no $G_{q-\gamma9}$ dissociation activity (BRET assay). (**D**) Comparison of the binding poses between lumateperone and IHCH-7086 at 5-HT$_{2A}$R, showing IHCH-7086's 2-methoxyphenyl moiety wedged between TM5 and TM6. In (A) and (C), error bars represent SEM (n = 3).

We previously reported that differences in ligand recognition in the EBP, specifically at TM7, result in divergent effects on ligand bias at 5-HT$_{2B}$R, especially for β-arrestin signaling (*19*, *20*). We hypothesized that the serotonin and psilocin binding pose that occupies the EBP in 5-HT$_{2A}$R would modulate β-arrestin signaling. We measured the β-arrestin2 recruitment activity caused by monoolein in the presence or absence of serotonin and found that monoolein can dose-dependently activate 5-HT$_{2A}$R–mediated β-arrestin signaling in the presence of serotonin in wild-type 5-HT$_{2A}$R but not in the G238$^{5.42}$S mutant where binding of serotonin to the bottom of the OBP is inhibited (Fig. 2C and fig. S3F). In the absence of serotonin, monoolein only shows modest G protein partial agonism, without detectable β-arrestin activity (Fig. 1C and fig. S1C). By contrast, monoolein did not activate the 5-HT$_{2A}$R–mediated β-arrestin activity in the presence of LSD (Fig. 2C). These results are consistent with serotonin and psilocin adopting a second binding pose in 5-HT$_{2A}$R and suggest that their interaction with EBP appears essential for monoolein-induced β-arrestin signaling.

To obtain further insight into the roles of the EBP in 5-HT$_{2A}$R–mediated β-arrestin2 recruitment, we solved the x-ray structures of the 5-HT$_{2A}$R–lisuride and 5-HT$_{2A}$R–LSD complexes to a resolution of 2.6 Å for both (table S1). The relatively high-resolution density maps of the two complexes allowed us to unambiguously assign the bound compounds and residues (Fig. 1B and fig. S1A). The overall structure of LSD-bound 5-HT$_{2A}$R is similar to the recently reported 3.4-Å structure (*23*), with root mean square deviation values of 0.81 Å for the C_α atoms of the receptor (fig. S4, A and B). A ~1- to 2-Å shift in the binding mode of LSD in our structure compared with the previous structure (fig. S4, A and B) may be attributed to the structures' different resolutions. A comparison of the LSD- or lisuride-bound 5-HT$_{2A}$R with the same ligand-bound 5-HT$_{2B}$R structures also shows that the overall orientation is similar (fig. S4, C to F). However, the binding mode of lisuride in 5-HT$_{2A}$R revealed a subtly different positioning of the (*S*)-diethylurea at the EBP of the receptor (fig. S4F).

We have previously shown that LSD's diethylamide, which is the key to LSD's potent hallucinogenic effects, contacts TM3 and TM7 within the EBP (*19*). Furthermore, we found that recognition of LSD in this region is stereoselective, because LSD's potent agonism was recapitulated only by the conformationally restricted (*S*,*S*)-azetidine stereoisomer. Surprisingly, in our 5-HT$_{2A}$R structure, the (*S*)-diethylurea of lisuride recapitulated the conformation of the diethylamide of LSD in the LSD–5-HT$_{2A}$R and LSD–5-HT$_{2B}$R complexes rather than the conformation of the (*S*)-diethylurea observed in the lisuride–5-HT$_{2B}$R complex (fig. S4, B, D, and F). This likely explains why lisuride is not an agonist of 5-HT$_{2B}$R but is an agonist of 5-HT$_{2A}$R (*20*).

Alignment of the 5-HT$_{2A}$R–LSD and 5-HT$_{2A}$R–lisuride structures further shows

that the two ethyl groups of LSD contact residue Y370$^{7.43}$ (Y, tyrosine), which only interacts with one ethyl group of lisuride (Fig. 2D and fig. S4G). Consistent with the idea that the steric extrusion of Y370$^{7.43}$ may cause a slight rotation of the diethyl group of lisuride in the EBP versus that of LSD (Fig. 2D and fig. S4G), we found that Y370$^{7.43}$W substitution strongly increases the efficacy of lisuride's β-arrestin2 recruitment agonism (Fig. 2E), despite similar surface expression levels relative to the wild-type receptor (fig. S3E). By contrast, it only slightly increases lisuride's G_q-mediated signaling efficacy (Fig. 2F). The Y370$^{7.43}$W mutation likely reduces LSD's efficacy in G_q-mediated signaling and β-arrestin2 recruitment because the Y370$^{7.43}$ directly interacts with the two ethyl groups of LSD (fig. S4, H and I). Similar results were obtained by the orthogonal β-arrestin2 association and $G_{q\text{-}\gamma 9}$ dissociation BRET assays (fig. S4, J and K). We observed no substantial affinity changes of lisuride and LSD at the Y370$^{7.43}$W mutant relative to wild-type 5-HT_{2A}R (table S3). Taken together, our results show that LSD and lisuride occupy the OBP in a similar fashion yet exhibit different poses in the EBP. It appears that ligand engagement with TM7, especially with Y370$^{7.43}$ in the EBP, leads to an auxiliary mechanism of 5-HT_{2A}R–mediated β-arrestin signaling activation.

Structure-oriented synthesis of arrestin-biased compounds

We posited that targeting the EBP may enhance β-arrestin recruitment at 5-HT_{2A}R, facilitating identification of β-arrestin–biased ligands. The recently solved 5-HT_{2A}R–risperidone and 5-HT_{2C}R–ritanserin crystal structures provide a starting point for identifying suitable chemotypes that engage the EBP (*21*, *22*) (fig. S5A). The two 5-HT_{2A}R antagonists, risperidone and ritanserin, share the same deep binding pose at 5-HT_2 receptors, which is characterized by the fluorobenzisoxazol ring and 4-fluorophenyl group, respectively, occupying the hydrophobic deep binding pocket (*21*, *22*, *28*) (fig. S5A). The top site moiety of risperidone and ritanserin is located in the EBP and adopts a similar pose to the second binding pose of serotonin and psilocin (fig. S5, A and B). Our design strategy, therefore, was to identify rigid substructures that can target the EBP and mimic the second binding pose of serotonin and psilocin, without engaging the bottom hydrophobic deep binding pocket that is responsible for antagonist activity. Because atypical antipsychotics are also 5-HT_{2A}R antagonists and share a similar embedded 4-fluorophenyl group, we suspected that they may adopt the same deep binding pose at 5-HT_{2A}R. After analyzing all available 5-HT_{2A}R 4-fluorophenyl antipsychotics, we identified three rigid moieties that are possibly suitable for binding the EBP: IHCH-7113 (moiety from lumateperone), IHCH-7117 (moiety from spiperone), and IHCH-7125 (moiety from pimozide and benperidol), which we synthesized (fig. S5A). Of the three molecules tested, IHCH-7113 was a 5-HT_{2A}R agonist [inhibition constant (K_i) = 758.58 nM; Fig. 3A and table S5]. Interestingly, IHCH-7113 showed a weak preference for β-arrestin2 association over G_q signaling (bias factor = 1.52) relative to serotonin (Fig. 3A and table S5).

To explore whether the tetracyclic scaffold of IHCH-7113 occupied the EBP, we crystallized lumateperone in 5-HT_{2A}R and solved the 5-HT_{2A}R–lumateperone structure at 2.45-Å resolution (fig. S5, C and D, and table S1). Analysis of lumateperone's binding pose revealed that the tetracyclic core is oriented in the EBP and adopts a similar pose to the second binding pose of serotonin and psilocin (Fig. 3B and fig. S5, E and F). We validated lumateperone's binding pose by alanine mutagenesis of the contacting residues, most of which decreased lumateperone's affinity (table S4). Like the previously solved risperidone and ritanserin poses, lumateperone places the 4-fluorophenyl group in the deep hydrophobic binding pocket defined by the side chains of TM3, TM5, and TM7 (fig. S5D). The close contacts between the lumateperone's 4-fluorophenyl group and I163$^{3.40}$ and F332$^{6.44}$ (I, isoleucine) in the PIF (proline-isoleucine-phenylalanine) motif and the "toggle switch" W336$^{6.48}$ (fig. S5D) apparently prevent the rearrangements required for receptor activation and potentially explain the antagonist activity of lumateperone at 5-HT_{2A}R.

To further test the hypothesis that the contact between the 4-fluorophenyl group of lumateperone determines its antagonist activity at 5-HT_{2A}R (*29*), we synthesized two analogs of lumateperone: IHCH-7112 and IHCH-7120, with the linker group shortened by one carbon in both cases and additional removal of the fluorine atom for IHCH-7120 to potentially attenuate the contact with the 4-fluorophenyl group. As expected, IHCH-7112 and IHCH-7120 were modest 5-HT_{2A}R agonists and were arrestin-biased by factors of 6.70 and 12.76, respectively (fig. S5G and table S5). In the previously solved 5-HT_{2A}R–25CN-NBOH structure, the 2-hydroxyphenyl moiety of the 25CN-NBOH agonist engages with TM3, TM6, and TM7 and avoids the conserved TM5 serine (S239$^{5.43}$ and S242$^{5.46}$) in the SEP (fig. S6A). Inspired by this, we further modified the structure of IHCH-7112 by introducing 2-methoxy or 2-hydroxy substitutions on the terminal phenyl group and adjusting the length of the linker (fig. S6B). These analogs retain the major interactions of the tetracyclic scaffold with the EBP that determine arrestin bias, but their increased flexibility limits binding to the conserved TM5 serine in the SEP. With respect to serotonin, all six hybrid analogs displayed a bias for β-arrestin–mediated signaling at 5-HT_{2A}R (Fig. 3C, fig. S6C, and table S5), with the most potent analogs being IHCH-7079 and IHCH-7086 (K_i = 16.98 and 12.59 nM, respectively) (Fig. 3C and fig. S6C). Unlike the nonselective agonists serotonin, psilocin, LSD, and lisuride, IHCH-7079 and IHCH-7086 prefer to bind 5-HT_2 receptors among the serotonin and dopamine receptors (table S6).

To obtain a better understanding of the ligand bias at 5-HT_{2A}R, we solved the crystal structures of 5-HT_{2A}R in complex with IHCH-7086, which showed β-arrestin–mediated signaling without detectable G_q activity (Fig. 3C and table S5). The structures were obtained at 2.5 Å (table S1). The electron density map for IHCH-7086 was well resolved (fig. S6D). The overall differences between the IHCH-7086– and lumateperone-bound 5-HT_{2A}R structures are relatively subtle, as predicted (Fig. 3D). The major difference is a rightward shift of the 2-methoxyphenyl moiety of IHCH-7086 versus the 4-fluorophenyl moiety of lumateperone (Fig. 3D). The 2-methoxyphenyl moiety of IHCH-7086, avoiding the PIF motif, drives close to F243$^{5.47}$, F244$^{5.48}$, and F340$^{6.52}$, consequently relocating three phenylalanines, which may explain the agonist activity of IHCH-7086 (Fig. 3D and figs. S5F and S6E). We also validated IHCH-7086's binding pose by alanine mutagenesis of contacting residues, most of which decreased IHCH-7086's affinity (table S4 and fig. S6F). As mentioned above, monoonlein, which contacts the conserved TM5 serine (S239$^{5.43}$ and S242$^{5.46}$) related to the SEP, only shows modest G protein partial agonism, without detectable β-arrestin activity (Fig. 1C and fig. S1C). Finally, the 2-methoxyphenyl moiety does not interact with the conserved TM5 serine, which potentially explains the nondetectable G protein activity of IHCH-7086 at 5-HT_{2A}R (fig. S6F).

Effects of 5HT_{2A}R-mediated signaling on hallucination and antidepressant-like behavior

A century of research has demonstrated that the affinities of psychedelics for 5-HT_{2A}R strongly correlate with their psychoactive potencies (*30*, *31*). Animal behavioral models cannot precisely capture the perturbations of perception, cognition, and mood produced by psychedelics in humans. However, studies have demonstrated that the mouse head twitch response (HTR) strongly correlates with the production of psychedelic-induced hallucinations in humans (*3*). Lisuride lacks comparable psychoactive properties in humans and also fails to induce the HTR in mice (*32*, *33*). Previously, genetic deletion of β-arrestin2 was found to decrease responsiveness to L-5-hydroxytryptophan and LSD-induced HTR (*34*, *35*). However, 2,5-dimethoxy-4-iodoamphetamine hydrochloride

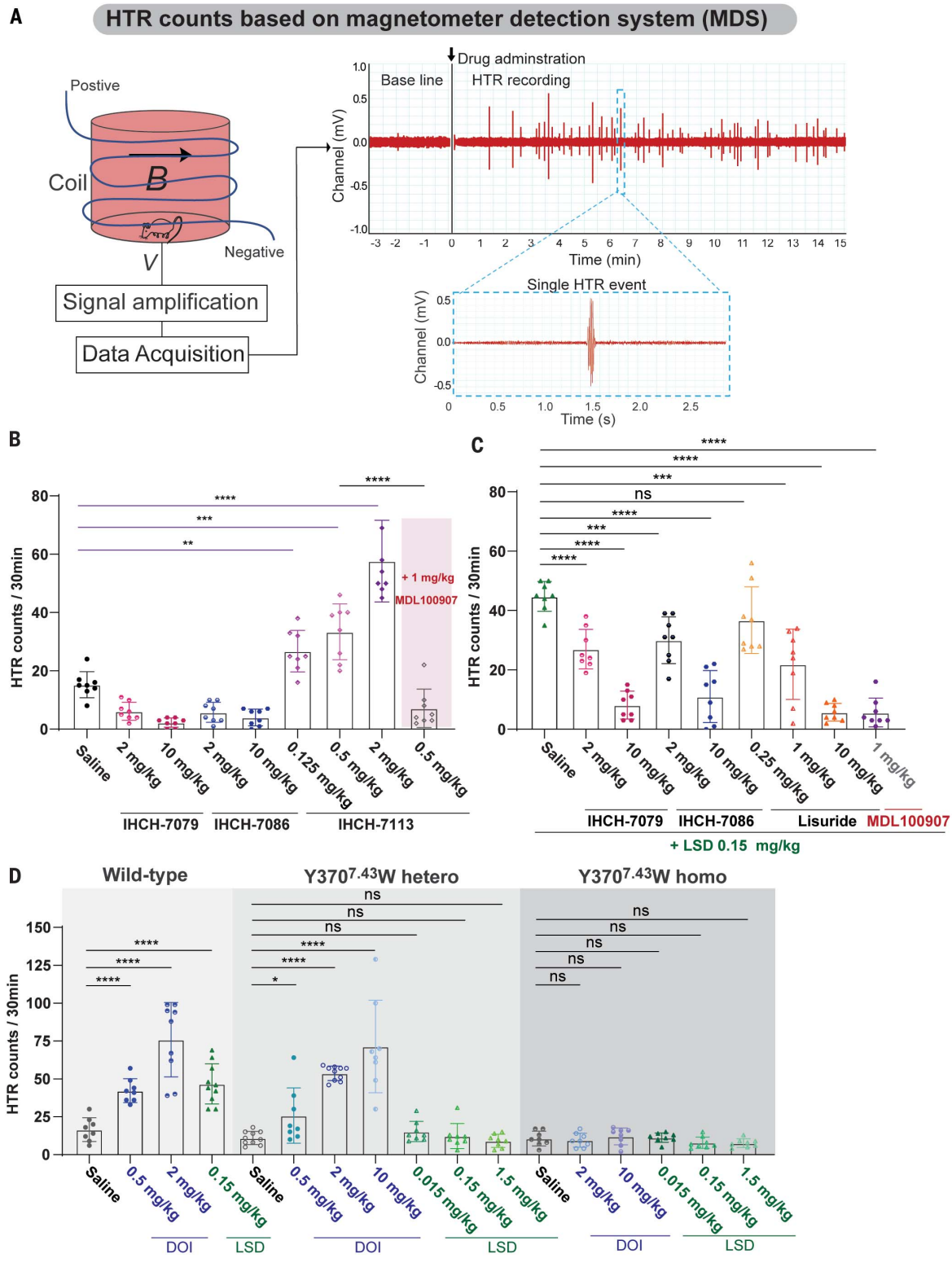

Fig. 4. Effects of the designed 5-HT$_{2A}$R agonists on animal behavior relevant to hallucination. (**A**) Scheme of the automated HTR detection system. A small magnet, surgically implanted on the mouse skull surface, produces an electrical signal of greater amplitude than background noise when the mouse displays an HTR. The signal is amplified and transduced by a data acquisition system. (**B**) IHCH-7113, not IHCH-7079 or IHCH-7086, induces a dose-dependent HTR in mice that is blocked by 5-HT$_{2A}$R selective antagonist MDL100907 (30- to 60-min time interval; see related fig. S8, E to G). (**C**) LSD-induced HTR is blocked by IHCH-7079, IHCH-7086, lisuride, and MDL100907 (60- to 90-min time interval; see related fig. S8H). (**D**) Effect of LSD and DOI on HTR behavior in 5-HT$_{2A}$R wild-type, Y370$^{7.43}$W-heterozygous, and Y370$^{7.43}$W-homozygous mice (0- to 30-min time interval; see related fig. S9). In (B) to (D), error bars represent SEM (n = 8 to 10 C57/BL6J or B6D2F1 mice). ns is not significant, *P < 0.05, **P < 0.01, ***P < 0.001, and ****P < 0.0001 (two-tailed unpaired Student's t test).

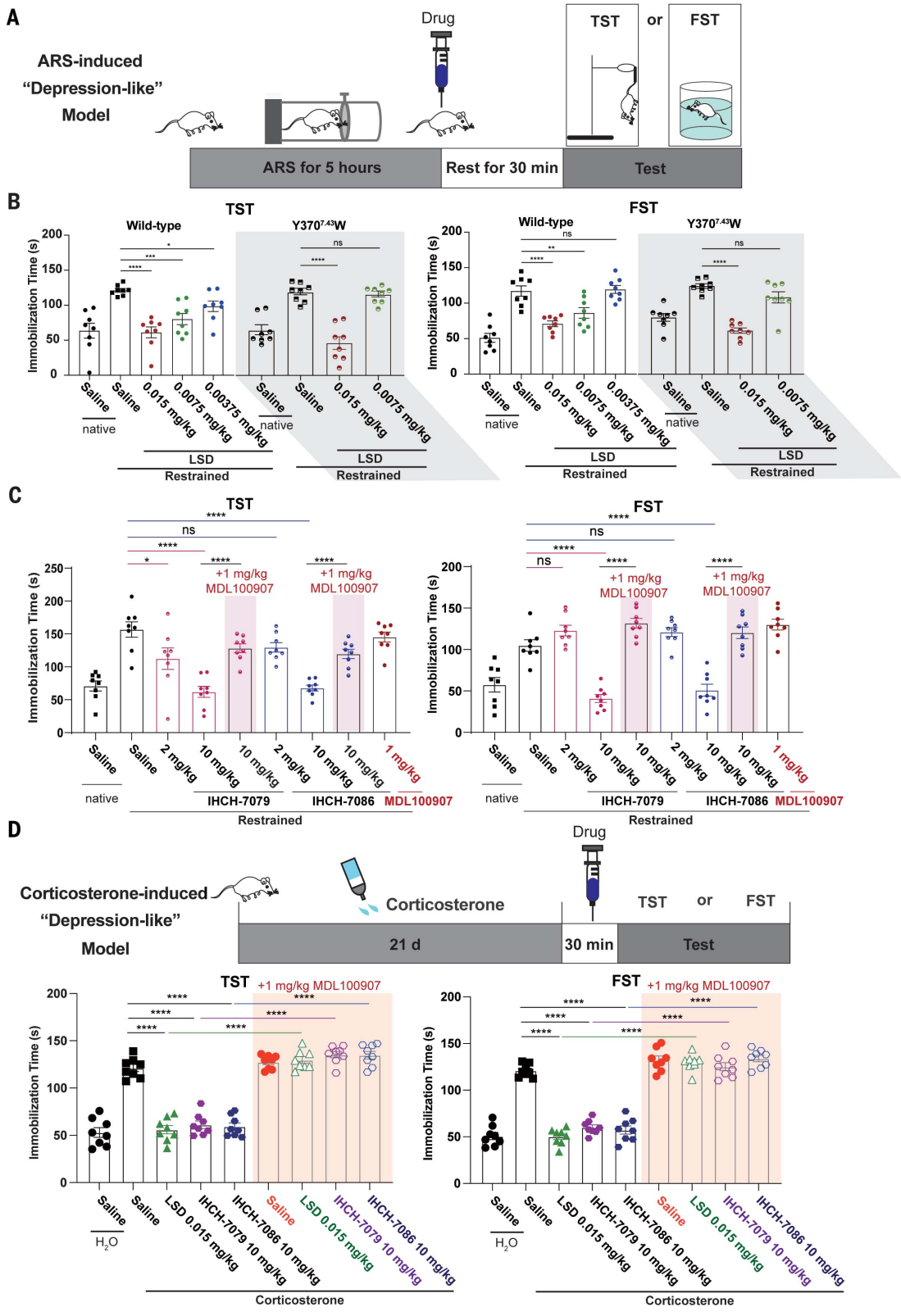

Fig. 5. The antidepressant effects of the designed 5-HT_{2A}R agonists on animal behavior relevant to depression. (**A**) Scheme of the ARS-induced depression-like model. (**B**) Effects of LSD on freezing behavior in ARS-induced depression-like mice in 5-HT_{2A}R wild-type and $Y370^{7.43}$W-homozygous mice. (**C**) Effects of IHCH-7086 and IHCH-7079 on freezing behavior in ARS-induced depression-like mice that are blocked by MDL100907. (**D**) Scheme of corticosterone-induced depression-like model. Effects of LSD, IHCH-7079, and IHCH-7086 on freezing behavior in corticosterone-induced depression-like mice that are blocked by MDL100907. The freezing behavior of mice was tested by the TST and FST. In (B) to (D), error bars represent SEM (n = 8 C57/BL6J or B6D2F1 mice). ns is not significant, *P < 0.05, **P < 0.01, ***P < 0.001, and ****P < 0.0001 (two-tailed unpaired Student's t test).

(DOI), another commonly used psychedelic that shows greatly attenuated HTR in G_q knockout mice (*36*), produced an HTR of equal magnitude in wild-type and β-arrestin2 knockout mice (*37*).

To test what intracellular signaling is required for the effects of psychedelics, we studied psychedelics (LSD, DOI, and psilocin), the nonhallucinogenic psychedelic analog (lisuride), and 5-HT_{2A}R arrestin-bias ligands (IHCH-7113, IHCH-7079, and IHCH-7086) for their ability to induce HTR in mice as detected by a fully automated magnetometer-based detection system (MDS) (Fig. 4A). As expected, the psychedelics (LSD, DOI, and psilocin), but not

lisuride, induced a significant HTR in mice (figs. S7A and S8, A to D). To our surprise, IHCH-7079 and IHCH-7086 failed to produce any HTR, even at doses as high as 10 mg/kg, unlike IHCH-7113, which produced HTR at doses as low as 0.125 mg/kg (Fig. 4B and fig. S8, E to G). However, the IHCH-7113–induced HTR was abolished by the 5-HT_{2A}R selective antagonist MDL100907. In mouse pharmacokinetic studies, IHCH-7113, IHCH-7079, and IHCH-7086 showed a reasonable half-life and excellent brain penetration properties (fig. S7B). Furthermore, LSD-induced HTR was not only abolished by the 5-HT_{2A}R selective antagonist MDL100907 but was also abolished by the nonhallucinogenic psychedelic analogs lisuride, IHCH-7079, and IHCH-7086 (Fig. 4C and fig. S8H).

Next, we analyzed the transduction efficiency of hallucinogenic psychedelics (DOI, LSD, psilocin, and IHCH-7113) and their nonhallucinogenic analogs (lisuride, IHCH-7079, and IHCH-7086) in G protein signaling and β-arrestin association at 5-HT_{2A}R by summarizing their relative $\log(\tau/K_A)$ values in a heat map (figs. S7C and S9) (τ, the efficacy of the agonist in the given pathway; K_A, the functional dissociation constant for the agonist). All tested psychedelics exhibited higher relative $\log(\tau/K_A)$ values than nonhallucinogenic analogs (fig. S7C). The above-mentioned data showed that the $Y370^{7.43}W$ mutation significantly reduced LSD's transduction efficiency for both β-arrestin recruitment and G protein signaling (fig. S4, H to J). Similar effects were observed for LSD and DOI activity on the mouse wild-type 5-HT_{2A}R and its $Y370^{7.43}W$ mutation (fig. S7D). In $Y370^{7.43}W$ mutant heterozygous mice, DOI induced HTR but LSD did not, whereas in homozygous mice, neither induced HTR (Fig. 4D and fig. S10). No significant differences were observed for 5-HT_{2A}R expression between wild-type and $Y370^{7.43}W$ littermates (fig. S7E). These data suggest that the psychoactive effects of psychedelics require a high transduction efficiency in 5-HT_{2A}R–mediated signaling.

Hallucinogens like psilocybin and LSD have been described to have potential therapeutic effects for depression (*2*). As shown in fig. S7F, acute administration of LSD [0.0075 and 0.015 mg/kg intraperitoneally (ip)] significantly attenuated acute restraint stress (ARS)–induced "depression-like" freezing behavior in the forced swimming test (FST) and tail suspension test (TST) (Fig. 5A). We further validated that acute administration of LSD (0.015 mg/kg ip) had antidepressant effects on 5-HT_{2A}R $Y370^{7.43}W$ mutant mice in the ARS-induced depression-like model (Fig. 5B). Given that there is no HTR activity induced by 0.015 mg/kg LSD in wild-type mice (fig. S7A) or 5-HT_{2A}R $Y370^{7.43}W$ mutant mice (Fig. 4D), it seems that the hallucinogenic effect may not be required for the antidepressant-like effect of LSD, consistent with a clinical trial of its microdose usage as an antidepressant (*2*). Because lisuride, IHCH-7079, and IHCH-7086 are not predicted to produce hallucinations (Fig. 4A and fig. S7A), we were interested in assessing their antidepressant potential in vivo. As shown in Fig. 5C and fig. S7F, acute administration of lisuride, IHCH-7079, and IHCH-7086 also significantly attenuated ARS-induced depression-like freezing behavior in the FST and TST, and the antidepressant-like effect of IHCH-7079 and IHCH-7086 was abolished by the 5-HT_{2A}R selective antagonist MDL100907 (Fig. 5C). To further validate the antidepressant-like effect of IHCH-7079 and IHCH-7086, C57BL/6J mice were subjected to the corticosterone-induced animal model of depression (*38*) and then tested in the FST and TST. As expected, mice treated with corticosterone for 21 days showed an increase in immobility compared with vehicle treatment (Fig. 5D). Similar to LSD, IHCH-7079 and IHCH-7086 also reduced immobility in corticosterone-treated mice, and the effects were abolished by MDL100907 (Fig. 5D). These data suggest that the low efficacy of 5-HT_{2A}R arrestin-biased agonists such as IHCH-7079 and IHCH-7086 may be sufficient for antidepressant effects.

Discussion

By leveraging six new 5-HT_{2A}R crystal structures, we have been able to reveal the structural basis of the lipid activation on 5-HT_{2A}R and also uncover a second binding mode for serotonin and psilocin, thereby enabling structure-based design of β-arrestin–biased ligands. Although the precise mechanisms of action of psychedelics remain largely unclear, 5-HT_{2A}R agonism is essential for their psychedelic effects in humans (*2*, *3*). We find that although the β-arrestin activity of 5-HT_{2A}R agonists plays a key role in their antidepressant effects and that the activity correlates with the agonists contacting TM7 residues of the EBP, this β-arrestin activity is insufficient for inducing psychoactive actions. Previous studies in humans reported that a 50 to 70% 5-HT_{2A}R occupancy level was required for an intense psilocybin-induced psychological experience (*39*). Indeed, it seems that the hallucinogenic effect requires high transduction efficiency of 5-HT_{2A}R agonists at both G protein–mediated signaling and β-arrestin recruitment. By contrast, the low transduction efficiency of 5-HT_{2A}R β-arrestin–biased agonists with no hallucinogenic effects may be sufficient to achieve the antidepressive effects. Finally, given recent successes in leveraging crystal structures of G protein–coupled receptors for ligand discovery, we anticipate that the reported structures herein will accelerate the search for new psychedelics and nonhallucinogenic psychedelic analogs for treatment of neuropsychiatric diseases.

REFERENCES AND NOTES

1. M. Berger, J. A. Gray, B. L. Roth, *Annu. Rev. Med.* **60**, 355–366 (2009).
2. D. Nutt, D. Erritzoe, R. Carhart-Harris, *Cell* **181**, 24–28 (2020).
3. D. E. Nichols, *Pharmacol. Rev.* **68**, 264–355 (2016).
4. A. S. A. T. Shulgin, *PIHKAL: A Chemical Love Story* (Transform Press 1991).
5. A. S. A. T. Shulgin, *TIHKAL: The Continuation* (Transform Press 1997).
6. C. M. Reiff *et al*., *Am. J. Psychiatry* **177**, 391–410 (2020).
7. R. Carhart-Harris *et al*., *N. Engl. J. Med.* **384**, 1402–1411 (2021).
8. S. Ross *et al*., *J. Psychopharmacol.* **30**, 1165–1180 (2016).
9. R. L. Carhart-Harris *et al*., *Psychopharmacology* **235**, 399–408 (2018).
10. R. R. Griffiths *et al*., *J. Psychopharmacol.* **30**, 1181–1197 (2016).
11. J. P. Huidobro-Toro, R. A. Harris, *Proc. Natl. Acad. Sci. U.S.A.* **93**, 8078–8082 (1996).
12. E. A. Thomas, M. J. Carson, M. J. Neal, J. G. Sutcliffe, *Proc. Natl. Acad. Sci. U.S.A.* **94**, 14115–14119 (1997).
13. D. L. Boger, J. E. Patterson, Q. Jin, *Proc. Natl. Acad. Sci. U.S.A.* **95**, 4102–4107 (1998).
14. W. B. Mendelson, A. S. Basile, *Neuropsychopharmacology* **25**, S36–S39 (2001).
15. L. P. Cameron *et al*., *Nature* **589**, 474–479 (2021).
16. C. Dong *et al*., *Cell* **184**, 2779–2792.e18 (2021).
17. C. Wang *et al*., *Science* **340**, 610–614 (2013).
18. D. Wacker *et al*., *Science* **340**, 615–619 (2013).
19. D. Wacker *et al*., *Cell* **168**, 377–389.e12 (2017).
20. J. D. McCorvy *et al*., *Nat. Struct. Mol. Biol.* **25**, 787–796 (2018).
21. Y. Peng *et al*., *Cell* **172**, 719–730.e14 (2018).
22. K. T. Kimura *et al*., *Nat. Struct. Mol. Biol.* **26**, 121–128 (2019).
23. K. Kim *et al*., *Cell* **182**, 1574–1588.e19 (2020).
24. P. Xu *et al*., *Nature* **592**, 469–473 (2021).
25. Y. Zhuang *et al*., *Cell* **184**, 931–942.e18 (2021).
26. R. O. Dror *et al*., *Proc. Natl. Acad. Sci. U.S.A.* **108**, 18684–18689 (2011).
27. R. H. J. Olsen *et al*., *Nat. Chem. Biol.* **16**, 841–849 (2020).
28. S. Wang *et al*., *Nature* **555**, 269–273 (2018).
29. K. E. Vanover *et al*., *Neuropsychopharmacology* **44**, 598–605 (2019).
30. R. A. Glennon, M. Titeler, J. D. McKenney, *Life Sci.* **35**, 2505–2511 (1984).
31. B. Sadzot *et al*., *Psychopharmacology* **98**, 495–499 (1989).
32. J. González-Maeso *et al*., *Neuron* **53**, 439–452 (2007).
33. J. González-Maeso *et al*., *J. Neurosci.* **23**, 8836–8843 (2003).
34. C. L. Schmid, L. M. Bohn, *J. Neurosci.* **30**, 13513–13524 (2010).
35. R. M. Rodriguiz, V. Nadkarni, C. R. Means, Y.-T. Chiu, B. L. Roth, W. C. Wetsel, bioRxiv 2021.02.04.429772 [Preprint] (2021); https://doi.org/10.1101/2021.02.04.429772.
36. E. E. Garcia, R. L. Smith, E. Sanders-Bush, *Neuropharmacology* **52**, 1671–1677 (2007).
37. C. L. Schmid, K. M. Raehal, L. M. Bohn, *Proc. Natl. Acad. Sci. U.S.A.* **105**, 1079–1084 (2008).
38. S. L. Gourley, J. R. Taylor, *Curr. Protoc. Neurosci.* **49**, 9.32.1–9.32.11 (2009).
39. M. K. Madsen *et al*., *Neuropsychopharmacology* **44**, 1328–1334 (2019).

ACKNOWLEDGMENTS

The diffraction data were collected at the BL45XU of SPring-8 (JASRI proposals 2021A2746 and 2020A2605). We thank K. Hirata, Y. Nakamura, and K. Hasegawa for their help with data collection. The psilocin and LSD involved in this paper were provided by the drug reference materials laboratory of the Third Research Institute of the Ministry of Public Security (China). **Funding:** This work was funded by Ministry of Science and Technology of China grant 2020YFA0509102 (S.W.); National Natural Science Foundation of China grant 32071197 (S.W.); Strategic Priority Research Program of the Chinese Academy of Sciences grant XDB19020111 (S.W.); Shanghai Science and Technology Committee grant 19ZR1466200 (S.W.); Thousand Talents Plan-Youth (S.W.); Shanghai Rising-Star Program grant 20QA1410600 (S.W.); National Natural Science Foundation of China grants 22177074 and 81703361 (J.C.); Shanghai Science and Technology Committee grant 20S11901200 (J.C.); and Shanghai Municipal Government and ShanghaiTech University (J.C.). **Author contributions:** Conceptualization: S.W., J.C., D.C.; Methodology: D.C., J.Y., H.W., Z.L., X.L., L.H., J.Q., L.F., L.T., Z.C.; Investigation: D.C., J.Y., H.W., Z.L., S.W.; Funding acquisition: S.W., J.C.; Project administration: S.W., J.C., J.L.; Supervision: S.W., J.C.; Writing – original draft: S.W.; Writing – review and editing: S.W., J.C., J.L., D.C. **Competing interests:** The authors declare that they have no competing interests. **Data and materials availability:** The data presented in this paper are

tabulated in the main paper and in the supplementary materials. Coordinates and structure factors for the 5-HT_{2A}R complexes with serotonin, psilocin, LSD, lisuride, lumateperone, and IHCH-7086 ligands are deposited in the Protein Data Bank under accession codes 7WC4, 7WC5, 7WC6, 7WC7, 7WC8, and 7WC9, respectively. All materials are available upon request.

SUPPLEMENTARY MATERIALS

science.org/doi/10.1126/science.abl8615
Materials and Methods
Supplementary Text
Figs. S1 to S10
Tables S1 to S7

References (*40*–*49*)
MDAR Reproducibility Checklist
View/request a protocol for this paper from *Bio-protocol*.

10 August 2021; accepted 21 December 2021
10.1126/science.abl8615

Science

Structure-based discovery of nonhallucinogenic psychedelic analogs

Dongmei CaoJing YuHuan WangZhipu LuoXinyu LiuLicong HeJianzhong QiLuyu FanLingjie TangZhangcheng ChenJinsong LiJianjun ChengSheng Wang

Science, 375 (6579), • DOI: 10.1126/science.abl8615

Nonhallucinogenic psychedelic analogs

Psychedelic drugs such as lysergic acid diethylamide (LSD) and mushroom-derived psilocybin exert their effects by binding the serotonin 2A receptor (5-HT2AR). These drugs also have antidepressant effects, but the hallucinations they cause complicate their use as therapeutics. Cao *et al*. present structures of 5-HT2AR bound to psychedelic drugs, the endogenous ligand serotonin, and the nonhallucinogenic drug lisuride. The structures reveal ligand-receptor interactions that cause a bias toward arrestin recruitment. Based on these insights, the authors designed arrestin-biased ligands that displayed antidepressant-like activity in mice without hallucination effects. Arrestin recruitment alone is insufficient for antidepressant effects, but the low G-protein signaling of the arrestin-biased ligands appears to allow antidepressant effects without causing hallucination. —VV